Kinetics of the Reaction between Cyclopentylperoxy Radicals and HO_2

Mary A. Crawford,† Joseph J. Szente, and M. Matti Maricq*

Research Laboratory, Ford Motor Company, P.O. Box 2053, Drop 3083, Dearborn, Michigan 48121

Joseph S. Francisco

Department of Chemistry, Purdue University, West Lafayette, Indiana 47907-1397

Received: March 25, 1997; In Final Form: May 2, 1997[⊗]

The techniques of time-resolved UV spectroscopy and transient IR absorption are used to examine the kinetics of the c-$C_5H_9O_2$ + HO_2 reaction over the temperature range 214−359 K. Deconvolution of the UV spectra yield time-dependent concentrations of both the cyclopentylperoxy and HO_2 reactants; the transient IR experiments separately monitor HO_2. Fits of these data to the appropriate reaction model yield a rate constant of $k_{ro2+ho2} = (3.2^{+15}_{-1.1}) \times 10^{-13} e^{(1150\pm200)/T}$ cm^3 s^{-1} for the title reaction. This result is compared to the single previous study of c-$C_5H_9O_2$ + HO_2 kinetics, and the implications for the atmospheric chemistry of peroxy radicals are discussed. As part of the present study, a relative rate of $k_{cl+c5h10}/k_{cl+ch3oh} = (2.3 \pm 0.3)e^{(300\pm200)/T}$ has been measured for the reaction Cl + c-C_5H_{10} → c-C_5H_9 + HCl relative to Cl + CH_3OH → CH_2OH + HCl.

Introduction

Central to the tropospheric chemistry of hydrocarbon compounds is the fate of the various intermediates formed as a result of their atmospheric degradation. One important class of intermediate is the organic peroxy radical, RO_2, formed when the hydrocarbon is attacked by an OH radical and the hydrocarbon radical subsequently adds O_2, i.e.

$$RH + OH \rightarrow R + H_2O \quad (1)$$

$$R + O_2 \rightarrow RO_2 \quad (2)$$

The chemical degradation pathway of the RO_2 radical is largely dictated by levels of NO_x, other peroxy radicals, and HO_2 present in the surrounding atmosphere with which it can react. For example, the reaction of RO_2 with NO serves as an important removal mechanism for peroxy radicals and plays a key role in photochemical ozone formation in urban areas where NO_x levels are relatively abundant. However, when NO_x concentrations are reduced, as often found in rural and remote environments, the reaction of RO_2 with HO_2 takes on an important role in the atmospheric degradation of hydrocarbons.

Despite their atmospheric importance, the reactions of HO_2 with RO_2 radicals other than methylperoxy have until recently received only scant attention in the literature.[1,2] For purposes of atmospheric modeling, the oxidation pathways of nonmethane hydrocarbons (NMHC) are patterned after those of methane. Because there exist such a large variety of NMHC-derived peroxy radicals and due to the lack of detailed chemical information, their reactions are treated in atmospheric models using lumped or surrogate mechanisms to describe their reactivity.[3,4] Via the lumped mechanism, organic species are grouped together according to a common basis such as structure or functionality. This is predicated on the presumption that structurally similar compounds will react in a similar manner. In the case of RO_2 + HO_2 reactions, these are parametrized in atmospheric models according to kinetic data for the reactions of methylperoxy and ethylperoxy radicals with HO_2.[4]

In situations where there is a lack of kinetic data available, as has been the case for the reactions of RO_2 with HO_2, the method of lumping reactions[3] provides a means of accounting for the unstudied reactions. Another advantage of lumping chemical mechanisms is the reduction in the computational resources that it brings about. However, recent investigations of reactions for various non-methane peroxy radicals with HO_2 have yielded results that now question the validity of using the CH_3O_2 + HO_2 reaction to characterize the body of RO_2 + HO_2 reactions. As a consequence, the criteria for lumping this important class of reactions needs to be reevaluated.

The purpose of the present paper is to verify the steeper temperature dependence and generally larger rate constant found for the reaction of "larger" organic peroxy radicals (including neopentylperoxy,[5] cyclopentylperoxy,[6] cyclohexylperoxy,[6] and $(CH_3)_2C(OH)CH_2O_2$ radicals[7]) with HO_2 as compared to methylperoxy. The room temperature rate constants for the "larger" peroxy radicals are approximately 3 times faster than for the methylperoxy reaction, and the temperature dependence has typically an $E_a \sim -1300$ K as compared to an $E_a \sim -800$ K. The need for verifying this behavior arises from the following considerations: The first investigation[8] of the ethylperoxy reaction with HO_2 revealed the kinetics to be quite similar to the analogous methylperoxy reaction.[9,10] Recently, a reevaluation[11] of the $C_2H_5O_2$ + HO_2 rate constant, by the same group responsible for the preponderance of "larger" peroxy radical studies, contradicted the first work,[8] suggesting that also the ethylperoxy radical behaves toward HO_2 as a "larger" peroxy radical. Efforts to resolve the discrepancy concerning the $C_2H_5O_2$ + HO_2 reaction were undertaken in this laboratory.[12] The results supported the initial work by Dagaut et al.,[8] namely, showing a temperature dependence comparable to that of methylperoxy. Naturally, this situation raises the question of whether or not a similar discrepancy could exist for the other "larger" peroxy radicals.

The present paper extends the previous work on the c-$C_5H_9O_2$ + HO_2 reaction in three ways: First, time-resolved UV spectroscopy is employed to follow the reaction, allowing us

† On leave from Department of Chemistry, Purdue University.
* To whom correspondence should be addressed.
⊗ Abstract published in *Advance ACS Abstracts,* June 15, 1997.

S1089-5639(97)01070-0 CCC: $14.00

to deconvolute the total absorbance at each time into contributions from c-$C_5H_9O_2$, HO_2, and stable products. Previously, this was done by analyzing pairs of time-dependent absorption traces taken at two separate wavelengths in order to deduce the c-$C_5H_9O_2$ and HO_2 contributions.[6] Second, transient IR detection of HO_2 is utilized as a separate method of monitoring this species concentration versus time profile, thereby verifying the UV measurements. Third, the rate constant measurements are extended down from 249 to 214 K. We also report a measurement of the UV cross section of the cyclopentylperoxy radical, examine its self-reaction kinetics at room temperature, and provide temperature-dependent relative rate constants for the reaction of chlorine atoms with cyclopentane relative to methanol.

Experimental Section

The reaction between c-$C_5H_9O_2$ and HO_2 is interrogated using the methods of flash photolysis−time-resolved UV spectroscopy and transient IR absorption that have been previously detailed.[13−15] Generation of the desired peroxy radical reactants is accomplished by the photolysis of Cl_2 or F_2 in gas mixtures of either $Cl_2/CH_3OH/O_2$/c-C_5H_{10}/N_2 or $F_2/H_2/O_2$/c-C_5H_{10}/N_2. The given mixture flows through a temperature-controlled cylindrical cell having a diameter of 3.2 cm and a path length of 51 cm. Gas flow rates are controlled using Tylan flow controllers with the exception of Cl_2 and F_2 whose flow rates are controlled using needle valves. The desired total pressure is achieved through the addition of N_2 gas.

The Cl_2 or F_2 in the gas mixture is photolyzed by a 10 ns, 300−600 mJ pulse of 351 nm light from an excimer laser. The halogen atoms that are produced abstract hydrogen atoms from the hydrogen-containing precursor species; thus, cyclopentylperoxy radicals are formed via

$$\text{c-}C_5H_{10} + \text{Cl (or F)} \rightarrow \text{c-}C_5H_9 + \text{HCl (or HF)} \quad (3)$$

$$\text{c-}C_5H_9 + O_2 + M \rightarrow \text{c-}C_5H_9O_2 + M \quad (4)$$

Whereas the above reaction scheme is used for c-$C_5H_9O_2$ generation in all of the experiments reported herein, two different methods are used to form HO_2. Hydrogen gas is the precursor when fluorine photolysis is used to initiate the reaction; thus,

$$F + H_2 \rightarrow HF + H \quad (5)$$

$$H + O_2 + M \rightarrow HO_2 + M \quad (6)$$

The generation of F atoms requires that precautions be taken to avoid the formation of FO_2. The latter is known to exhibit a spectrum similar in shape to that of HO_2, but with several times the intensity. This problem is avoided by keeping the $[H_2]/[O_2]$ and $[C_5H_{10}]/[O_2]$ ratios sufficiently high to limit FO_2 production to less than 1% of the total number of radicals.

Initiation of the radical chemistry by F_2 photolysis is precluded at temperatures above ∼250 K due to a spontaneous chain reaction between the F_2 and c-C_5H_{10} precursors. Instead, Cl_2 photolysis is utilized. However, the reaction between Cl and H_2 is too slow to generate HO_2 on the desired time scale without the addition of an unduly large amount of hydrogen. Therefore, methanol is employed to form HO_2 via the reactions

$$CH_3OH + Cl \rightarrow CH_2OH + HCl \quad (7)$$

$$CH_2OH + O_2 \rightarrow CH_2O + HO_2 \quad (8)$$

Owing to methanol's low vapor pressure, however, this procedure cannot be employed at temperatures below 250 K.

Experimental conditions are set such that the generation of the peroxy radicals takes place within a few microseconds of the photolysis pulse, a time scale rapid compared to the 500 μs range of the subsequent peroxy radical reactions. The number of chlorine atoms generated by the photolysis pulse is determined separately by replacing the cyclopentane and the HO_2 precursors with ethane under otherwise identical experimental conditions and recording the number of ethylperoxy radicals that are generated. The total radical concentration varies from roughly 5×10^{14} to 8×10^{14} cm^{-3}. Over the course of the experiments, but not at each temperature, the ratio $[HO_2]/[\text{c-}C_5H_9O_2]$ is varied from about 0.5 to 2.5.

Time-resolved UV spectra of the reaction mixture are collected at delay times in the range 10−500 μs following the photolysis pulse. This is accomplished by passing broad-band UV light from a D_2 lamp longitudinally through the cell in a direction opposite the photolysis beam. The probe light is dispersed by a 0.32 m monochromator with a 147 groove/mm grating onto a gated diode array detector. This configuration allows the UV absorption of the peroxy radicals to be monitored over a wavelength range of 190−340 nm and at a time resolution of 10 μs. The spectra are deconvoluted into time-dependent concentrations according to

$$\text{Abs}(t) = [HO_2]_t\sigma(HO_2)l + [\text{c-}C_5H_9O_2]_t\sigma(\text{c-}C_5H_9O_2)l + [\text{products}]_t\sigma(\text{products})l \quad (9)$$

where l represents the path length and σ the wavelength-dependent cross section of the relevant species. The absolute UV cross section for HO_2 is reported in ref 12 and is in good agreement with the recommended spectrum;[1,2] the cyclopentylperoxy absorption cross section is remeasured in the present study. The last term in the deconvolution accounts for small contributions to the absorbance of the reaction mixture by long-lived products, predominantly HOOH and c-C_5H_9OOH.

In addition to the UV probe, the loss of HO_2 is separately monitored using transient IR spectroscopy.[15] This is accomplished by recording, after the photolysis pulse, the change in light intensity of a Pb salt diode laser beam that counterpropagates through the experimental cell in place of the broad-band UV light. The HO_2 radical is monitored by a vibration−rotation line in the ν_3 O−O stretch band that conveniently falls between a pair of ammonia lines at 1117.45 and 1117.64 cm^{-1}. Since the HO_2 radical is a short-lived species, this coincidence simplifies locating the absorption line.[16]

The IR light intensity is monitored by a HgCdTe detector with a 0.3 μs response time. This is an ac coupled device that is sensitive only to changes in light intensity and not the absolute level. It has a decay constant of $k_{det} = 300$ s^{-1} that over the 1 ms time scale of the present experiments makes a small contribution to the signal attributable to the changing HO_2 concentration. Thus, the HO_2 concentration is ascertained using the following modified form of Beer's law:

$$\frac{dV(t)}{dt} = V_0 \frac{d}{dt} e^{-[HO_2]_t\sigma_{ho2}l} - k_{det}V(t) \quad (10)$$

Here, $V(t)$ represents the detector signal, k_{det} is the detector time constant, l is the path length, and σ_{ho2} is the IR cross section of the probe vibration−rotation line. The IR cross section, which depends on temperature and pressure, is measured by generating a known amount of the radical via Cl_2 photolysis in a methanol/oxygen mixture. The "known" amount is calibrated against the quantity of $C_2H_5O_2$ produced upon substitution of ethane for methanol.

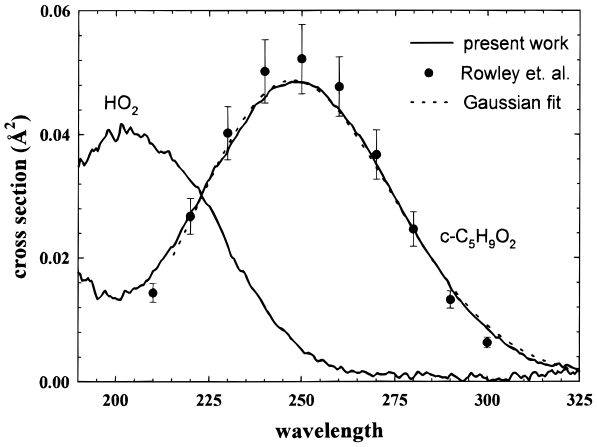

Figure 1. UV absorption spectrum of c-$C_5H_9O_2$. The spectrum recorded in the present study is given by the solid line. The dashed line represents a fit of the 250 nm band to a Gaussian line shape. The symbols represent results from ref 17. The spectrum of HO_2 from ref 12 is provided for comparison.

The experimental measurements are performed over the temperature range 214−360 K. Temperature control is maintained by a Neslab ULT-80dd recirculating chiller that precools/preheats the gases, with the exception of cyclopentane, before entrance into the experimental cell. The cyclopentane (99%) and methanol (99.9%) are acquired from Fisher. Nitrogen (99.999%), oxygen (ultrazero grade, THC <0.5 ppm), ethane (99.5%), and hydrogen (47.8% in nitrogen) are purchased from Michigan Airgas. Chlorine (9.7% or 4.8% in nitrogen) and fluorine (10% in nitrogen) are obtained from Matheson. All the reagents are used without further purification.

c-$C_5H_9O_2$ UV Spectrum and Self-Reaction

Cyclopentylperoxy radicals are generated by Cl_2 photolysis followed by reactions 3 and 4 in a gas mixture composed of c-$C_5H_{10}/O_2/Cl_2/N_2$. In order to ensure quantitative conversion of the Cl atoms to c-$C_5H_9O_2$ radicals, the absorbance of the reaction mixture is measured as a function of the concentrations of cyclopentane and oxygen. The formation of the peroxy radical shows little dependence on the concentrations of c-C_5H_{10} and O_2 when [c-C_5H_{10}] > 0.1 Torr and [O_2] > 10 Torr. Consistent with the very rapid reaction between c-C_5H_{10} and Cl is the low amount of c-C_5H_{10} required for quantitative conversion of the chlorine atoms to the peroxy radicals.

The UV spectrum of c-$C_5H_9O_2$, shown in Figure 1, consists of a broad unfeatured band typical of peroxy radicals centered at about 250 nm, as well as indications of a second band beginning below 215 nm. The intensity of the spectrum is placed on an absolute scale by substituting ethane for cyclopentane under otherwise identical conditions and measuring the $C_2H_5O_2$ concentration produced from

$$Cl + C_2H_6 \rightarrow C_2H_5 + HCl \qquad (11)$$

$$C_2H_5 + O_2 + M \rightarrow C_2H_5O_2 + M \qquad (12)$$

using the well-characterized absorption cross section of $C_2H_5O_2$.[1,2,13] The ethylperoxy concentration is equated to the initial Cl atom concentration and thereby the initial cyclopentylperoxy concentration. Each measured spectrum was extrapolated to $t = 0$ to correct for any loss of peroxy radicals which may have occurred as a result of self-reaction.

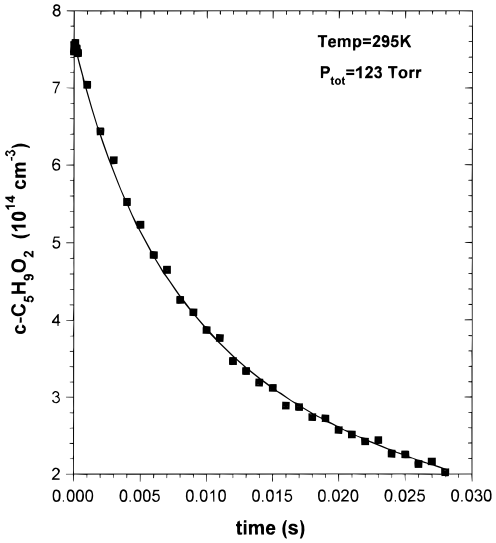

Figure 2. Concentration versus time profile for the self-reaction of c-$C_5H_9O_2$.

The maximum cross section and corresponding wavelength of the principal absorption band are found by fitting the UV spectrum above 215 nm to a Gaussian line shape,

$$\sigma = \sigma_{max} \exp(-b[\ln(\lambda_{max}/\lambda)]^2) \qquad (13)$$

where $\lambda_{max} = 248$ nm, $\sigma_{max} = 0.049$ Å^2, and $b = 45$. Figure 1 shows the present measurement to be in very good agreement with the previous work reported by Rowley et al.[17] Both spectra peak near 250 nm. The estimated uncertainty in the cross section reported here is 10%, which includes a 5% uncertainty in the $C_2H_5O_2$ calibration spectrum and 5% due to possible changes in experimental conditions when substituting ethane for cyclopentane.

Time-resolved spectra of the c-$C_5H_9O_2$ radical show its absorption to decay slowly. Each spectrum is converted into a concentration by comparison to the reference spectrum of the cyclopentylperoxy radical. The concentration versus time profiles are subsequently fit to a second-order decay appropriate for the reaction

$$\text{c-}C_5H_9O_2 + \text{c-}C_5H_9O_2 \rightarrow \text{products} \qquad (14)$$

Figure 2 shows the data along with the best fit, corresponding to a room temperature rate constant of $k_{14obs} = 6.3 \times 10^{-14}$ cm^3 s^{-1}. This "observed" rate constant includes secondary removal of $C_5H_9O_2$, principally by reaction with HO_2 formed from the products of reaction 14; thus, it may vary depending on the conditions under which it is measured. In this case, however, the present result is identical to the value of 6.3×10^{-14} cm^3 s^{-1} recorded by Rowley et al.[17] It verifies that removal of c-$C_5H_9O_2$ by self-reaction is very slow. Thus, in experiments where both HO_2 and c-$C_5H_9O_2$ are present, the principal radical loss channels are via self-reaction of HO_2 and the cross-reaction between HO_2 and c-$C_5H_9O_2$; the cyclopentylperoxy self-reaction plays only a minor role.

The c-$C_5H_9O_2$ + HO_2 Reaction

Figure 3 illustrates the variation in time of the reaction mixture's UV absorbance that is typical after photolysis when precursors for both c-$C_5H_9O_2$ and HO_2 are present. Comparison with the reference spectra of cyclopentylperoxy and HO_2 (Figure 1) reveals that the initial absorption maximum of the reaction mixture falls somewhere between the absorption peaks of these

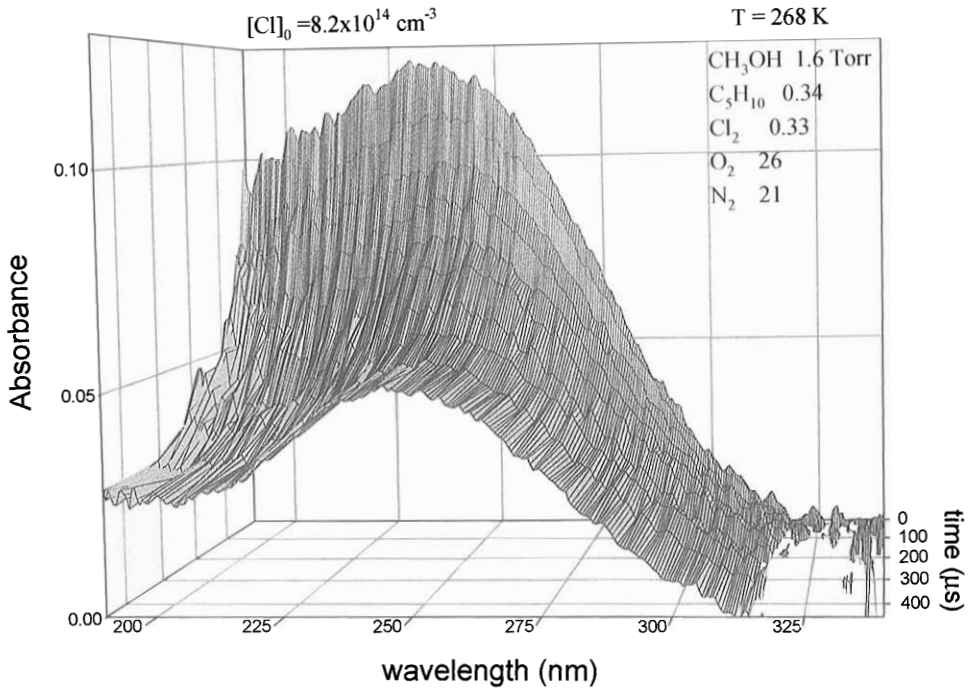

Figure 3. UV absorption−wavelength−time surface for the c-$C_5H_9O_2$ + HO_2 reaction. Experimental conditions correspond to those of experiment 7 of Table 2. The slightly negative absorbance around 325 nm is due to Cl_2 loss from photolysis.

two species. This is consistent with a convoluted spectrum composed of two distinct broadly absorbing species. As the reaction proceeds, the overall intensity of the absorbance decreases with time due to the loss of both c-$C_5H_9O_2$ and HO_2.

The removal of the cyclopentylperoxy radical predominantly occurs via its reaction with HO_2,

$$HO_2 + \text{c-}C_5H_9O_2 \rightarrow \text{c-}C_5H_9OOH + O_2 \qquad (15)$$

since the self-reaction of cyclopentylperoxy is too slow to be a factor in the current measurements. This is apparent from the difference in time scales between Figures 2 and 3. The disappearance of the HO_2 radical is due both to reaction 15 and the self-reaction

$$HO_2 + HO_2 \rightarrow H_2O_2 + O_2 \qquad (16)$$

Consequently, HO_2 is lost more rapidly than c-$C_5H_9O_2$, which explains the shift, in Figure 3, of the peak in the absorbance to the red as time increases. At longer times, the spectrum approaches that of the cyclopentylperoxy radical, except at wavelengths below ~215 nm, at which the absorbance is higher than expected.

The additional absorbance at short wavelengths is due to the hydroperoxy compounds formed in reactions 15 and 16. The UV spectrum of H_2O_2 begins gaining strength below about 225 nm, with an intensity in this region roughly 1/10 that of HO_2.[18] The spectrum of c-C_5H_9OOH is unknown, but it is expected to be similar to that of H_2O_2. Because these species absorb in roughly the same spectral region as HO_2, they can interfere with determination of $[HO_2]_t$. For this reason, the deconvolution procedure, eq 9, includes a term to account for absorption by these products, with σ(products) obtained from spectra taken a long time (20 ms) after photolysis.

Deconvolution of the time-resolved spectra is achieved by fitting them to eq 9, treating $[HO_2]_t$, $[\text{c-}C_5H_9O_2]_t$, and $[\text{products}]_t$ as adjustable parameters. The actual reference spectra are used for this purpose and not the Gaussian fits. Figure 4 provides examples of typical concentration versus time profiles obtained for the peroxy radicals in this manner. Initially, the c-$C_5H_9O_2$ concentration falls off rapidly, owing to its reaction with HO_2. Once the HO_2 radicals have disappeared, however, c-$C_5H_9O_2$ loss occurs at a much slower rate via its self-reaction.

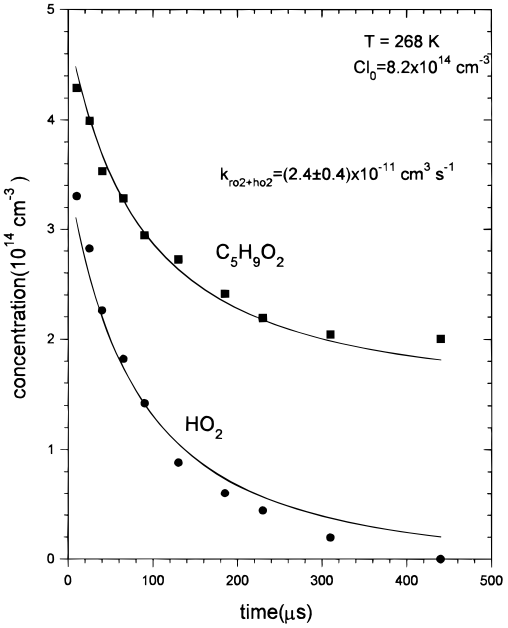

Figure 4. Concentration versus time profiles for the c-$C_5H_9O_2$ + HO_2 reaction. Concentrations are obtained by deconvolution of the spectra composing Figure 3.

The loss of HO_2, as measured by its transient IR absorption, is illustrated in Figure 5. For most of the IR measurements, a corresponding time-resolved UV experiment was carried out employing very nearly the same radical concentrations, except at a total pressure of about 50 Torr. The lower total pressure was used to enhance sensitivity, since the IR line intensity is inversely proportional to the pressure of the bath gas. For these pairs of experiments, the UV- versus IR-derived values of $k_{ro2+ho2}$ are in very good agreement.

The concentration versus time data, whether from UV or IR measurements, are fit to the kinetic model shown in Table 1,

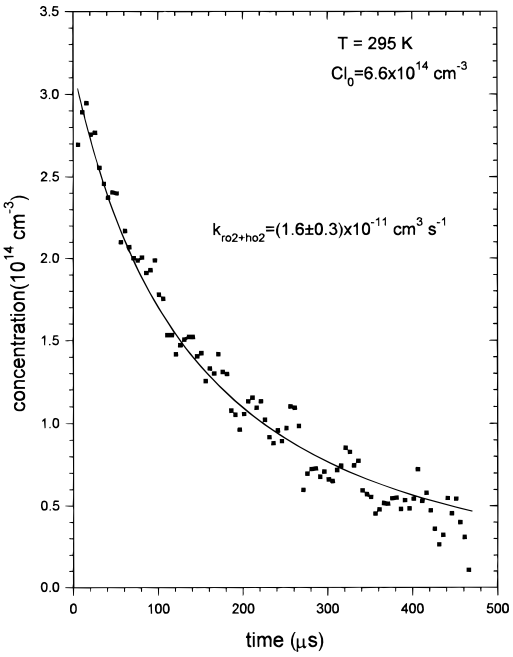

Figure 5. HO_2 concentration versus time as obtained from transient IR absorption by the ν_3 O−O stretch. Experimental conditions correspond to those of experiment 10′ of Table 2.

TABLE 1: c-$C_5H_9O_2$ + HO_2 Reaction Mechanism

reaction[a]	rate constant k
16. $HO_2 + HO_2 \rightarrow H_2O_2 + O_2$	$2.8 \times 10^{-13} e^{594/T}$ cm^3 s^{-1} [12]
14. c-$C_5H_9O_2$ + c-$C_5H_9O_2 \rightarrow$ products	6.3×10^{-14} cm^3 s^{-1} [b]
15. c-$C_5H_9O_2 + HO_2 \rightarrow$ c-$C_5H_9OOH + O_2$	$3.2 \times 10^{-13} e^{1150/T}$ cm^3 s^{-1} [c]

[a] Reaction numbers correspond to those used in text. [b] Value determined at 295 K; present and literature[6] relative rate measurements indicate the rate constant to be nearly temperature independent. [c] Measured in present study.

consisting of the RO_2 and HO_2 self-reactions and their cross-reaction. The best fits of the data to this model are indicated by the solid lines in Figures 4 and 5, and the corresponding rate constants are listed in Table 2. The fitting procedure involves two adjustable parameters: the first is $k_{ro2+ho2} \equiv k_{15}$, the rate constant of the cross reaction, and the second parameter is defined as the difference in the initial concentrations of HO_2 and c-$C_5H_9O_2$. The total initial radical concentration is determined independently by the ethylperoxy substitution procedure described in the Experimental Section. That the concentrations of c-$C_5H_9O_2$ and HO_2 can be fit simultaneously indicates that the data are internally consistent.

Several factors contribute to the error in k_{15}, such as the value of the initial concentrations of HO_2 and c-$C_5H_9O_2$ as well as uncertainties in the self-reaction rate constants. Ten percent uncertainties in the initial concentrations $[HO_2]_0$ and $[c\text{-}C_5H_9O_2]_0$, which arise from the optical cross sections used in their determination, result in 7% contributions to the error in the best fit value of k_{15}. Uncertainties due to the self-reaction rate constants of HO_2 and c-$C_5H_9O_2$ affect the best fit value of k_{15} to only a few percent. The principal source of error is from noise in the concentration versus time profiles, which ranges from 10 to 25%. Combining these contributions statistically, the total uncertainty in k_{15} ranges from ±15 to ±30%.

The temperature dependence of the c-$C_5H_9O_2$ + HO_2 rate constant is shown in Figure 6 and is compared with the results published by Rowley et al.[6] The rate constants along with the experimental conditions are listed in Table 2. The slight discrepancies between this work and the previous study are well within the error bounds of each study. Our results are best described by the following Arrhenius expression:

$$k_{15} = (3.2^{+1.5}_{-1.1}) \times 10^{-13} e^{(1150 \pm 200)/T} \quad \text{cm}^3\,\text{s}^{-1} \qquad (17)$$

The negative temperature dependence is typical of $HO_2 + RO_2$ reactions and is suggestive of the reaction passing through a rate-limiting intermediate complex.

It may be noticed, in Figure 6, that three of the five rate constant determinations utilizing F_2 photolysis and H_2 to generate HO_2 appear on the verge of being systematically lower than the remaining data. We do not believe these data to be sufficiently statistically significant to warrant concern that there is a systematic difference arising from the two methods of

TABLE 2: $C_5H_9O_2$ + HO_2 Rate Constants

			p, Torr						
exp no.[c]	temp, K	P_{tot}, Torr	C_5H_{10}	F_2 or Cl_2	O_2	HO_2 precursor[a]	$[HO_2]_0$, 10^{14} cm^{-3}	$[C_5H_9O_2]_0$, 10^{14} cm^{-3}	results[b] k_7, 10^{-11} cm^3 s^{-1}
1	214	155	0.81	4.9	79	12*	2.7	3.2	6.6 ± 1.4
2	214	159	0.92	5.4	89	7.7*	2.0	4	4.7 ± 1.3
3	225	159	0.94	4.7	97	6.7*	1.4	3.9	4.3 ± 1.0
4	231	163	0.80	5.2	83	13*	3.4	3.0	3.6 ± 0.8
5	253	159	0.88	5.2	88	8.7*	1.9	3	4.0 ± 0.8
6	267	50	0.22	0.36	27	1.6	4.1	3.9	2.7 ± 0.4
6′	267	50	0.22	0.36	27	1.6	4.3	3.4	3.0 ± 0.6
7	268	49	0.34	0.33	26	1.6	3.4	4.8	2.4 ± 0.4
7′	268	49	0.34	0.33	26	1.5	3.7	4.2	2.9 ± 0.5
8	271	137	0.14	0.35	28	2.0	3.7	2.0	3.0 ± 1.0
9	295	136	0.49	0.37	32	1.4	1.9	3.7	1.6 ± 0.4
10	295	48	0.34	0.31	26	1.5	2.8	4.3	1.8 ± 0.4
10′	295	49	0.34	0.31	26	1.5	3.0	3.6	1.6 ± 0.3
11′	324	52	0.25	0.37	28	1.7	4.2	3.3	1.0 ± 0.2
12	325	149	0.32	0.41	33	1.8	3.9	3.6	1.2 ± 0.2
13	356	50	0.18	0.43	38	2.3	5.0	1.8	0.6 ± 0.1
14	356	50	0.45	0.45	19	1.1	2.6	5.9	0.8 ± 0.2
15	357	50	0.18	0.44	38	2.3	5.7	2.5	0.7 ± 0.2
15′	357	50	0.18	0.44	38	2.3	5.1	3.0	0.7 ± 0.2
16	358	138	0.49	0.38	32	1.4	1.9	3.6	0.7 ± 0.2
17	359	142	0.32	0.41	32	1.7	3.6	3.7	0.8 ± 0.1

[a] HO_2 precursor is indicated as follows: asterisk represents H_2; the others are CH_3OH. When H_2 is used as the precursor, the chemistry is initiated by F_2 photolysis; for CH_3OH it is initiated by Cl_2 photolysis. [b] Error bars are $\pm 2\sigma$ and include systematic uncertainties. [c] Rate constant indicated by a prime determined from transient IR measurement of $[HO_2]$.

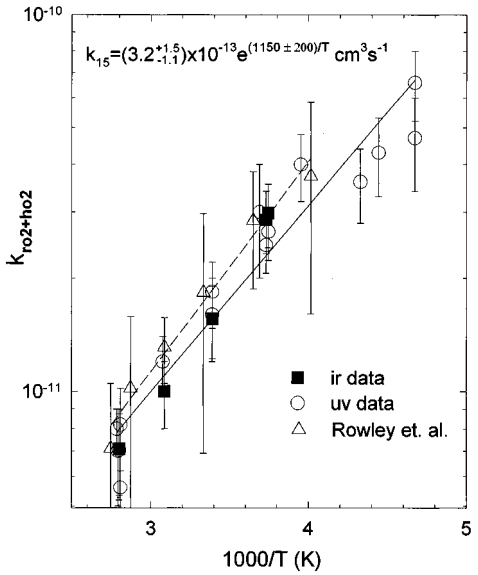

Figure 6. Temperature dependence of the c-$C_5H_9O_2$ + HO_2 reaction rate constant. Error bars are $\pm 2\sigma$ and for the present results include systematic uncertainties. The solid and dashed lines are linear regressions of the present data and those of Rowley et al.,[6] respectively.

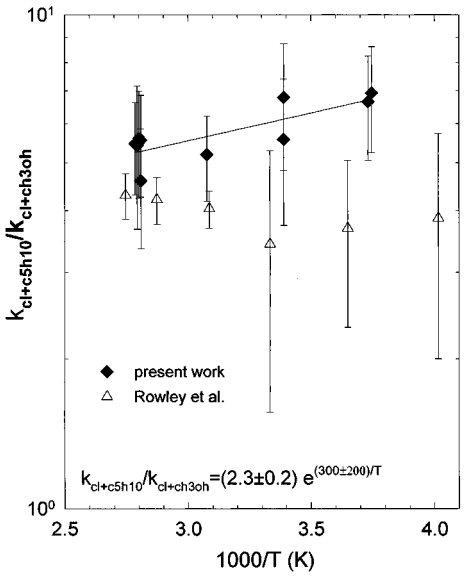

Figure 7. Temperature dependence of the Cl + c-C_5H_{10} versus Cl + CH_3OH relative reaction rate. Error bars are $\pm 2\sigma$. The data of Rowley et al. are from ref 6.

radical generation employed in these experiments. Instead, they are more likely to arise from difficulties associated with the low temperature and consequently low cyclopentane vapor pressure. Eliminating the lowest four temperature points changes the best fit Arrhenius expression from the one in eq 17 to $k_{15} = (1.2^{+0.8}_{-0.5}) \times 10^{-13}e^{(1450\pm200)/T}$ cm^3 s^{-1}, an expression that is within the error bounds of the original version.

Cl + c-C_5H_{10} versus Cl + CH_3OH Relative Rate

Formation of the peroxy radicals in the title reaction by Cl_2 photolysis in the presence of cyclopentane and methanol involves a competition for reaction with chlorine atoms by these two precursors. Thus, the ratio of initial peroxy radical concentrations is given by

$$\frac{[RO_2]_0}{[HO_2]_0} = \frac{k_3[C_5H_{10}]}{k_7[CH_3OH]} \qquad (18)$$

assuming that the O_2 reactions that follow Cl attack, reactions 4 and 8, are essentially instantaneous. Use of the data in Table 2 allows the inversion of eq 18 to recover the rate constant ratio k_3/k_7.

The values of $[HO_2]_0$ and $[RO_2]_0$ in Table 2 are obtained from the kinetic data as follows: The total radical concentration is measured by the corresponding ethylperoxy calibration, and the difference $[HO_2]_0 - [RO_2]_0$ is derived from fitting the time-dependent concentration traces to the mechanism of Table 1. Combining these with the initial precursor concentrations provides the rate constant ratios plotted versus temperature in Figure 7. A fit of these ratios to the Arrhenius form gives

$$k_{cl+c5h10}/k_{cl+ch3oh} = (2.3 \pm 0.2)e^{(300\pm200)/T} \qquad (19)$$

which shows a rather small negative temperature dependence. Neither of the reactions comprising this ratio has been much studied. The measurement by Lightfoot et al.[19] of the Cl + CH_3OH reaction relative to methane indicates it to be temperature independent over the 248−573 K range with $k_{cl+ch3oh} = 5.3 \times 10^{-11}$ cm^3 s^{-1}. Inserting this into eq 19 implies that the Cl + c-C_5H_{10} reaction is nearly temperature independent and that it has a room temperature rate constant of $k_{cl+c5h10}(298) = (3.3 \pm 0.7) \times 10^{-10}$ cm^3 s^{-1}. This conclusion is consistent with the relative rate measurements by Rowley et al.[6] that are compared in Figure 7 to our data and to the room temperature value of 3.3×10^{-10} cm^3 s^{-1} from the relative rate study of Wallington et al.[20]

Discussion

The present investigation of the c-$C_5H_9O_2$ + HO_2 reaction utilizes two methods to follow the reaction kinetics. One is time-resolved UV spectroscopy, in which complete spectra of the reaction mixture spanning the 190−325 nm range are gathered at a series of times following initiation of the reaction in order to extract the time dependence of the c-$C_5H_9O_2$ and HO_2 concentrations. Whereas conventional transient absorption measurement at two wavelengths is in principle sufficient to determine the concentrations of these two species, the present method by relying on a multitude of wavelengths more readily avoids systematic interferences such as may arise from weakly absorbing product species, electrical interference, scattered light, and other sources. A second method, namely transient IR absorption, is used to confirm the HO_2 concentrations deconvolved from the UV spectra. Unlike the broad overlapping UV spectra, the IR vibration−rotation lines are well-resolved, allowing unique detection of the HO_2 radical. The successful combination of these techniques increases the confidence in the $k_{ro2+ho2}$ measurements.

The current rate constant measurements support those made previously by Rowley et al.[6] For the c-$C_5H_9O_2$ + HO_2 system, absorption by the products is weak and limited to wavelengths below roughly 215 nm; thus, the measurements of Rowley et al. at 220 and 260 nm were relatively free from this source of interference, presumably leading to the good agreement with the present work. Both sets of rate constants (Figure 6) exhibit a relatively steep negative temperature dependence. As discussed above, the temperature dependence of $k_{ro2+ho2}$ can be determined in two ways depending on whether or not the data below 250 K are included. Over the entire 214−359 K range of the present measurements, the temperature dependence is characterized by $E_a = -(1150 \pm 200)$ K. Restricted to temperatures above 250 K, the "activation energy" increases to $-(1450 \pm 200)$ K. Either value is in good agreement with the earlier report[6] of $E_a = -(1323 \pm 185)$ K derived from data in the 249−364 K range.

The principal outcome of the present kinetic investigation is that the rate constant for the c-$C_5H_9O_2$ + HO_2 reaction has a different temperature dependence than does the analogous reaction between CH_3O_2 and HO_2 or, for that matter, $C_2H_5O_2$ and HO_2. The implication is that the reaction between methylperoxy radical and HO_2 cannot be used to embody RO_2 + HO_2 reactions in atmospheric models. Although the levels of non-methane hydrocarbons in unpolluted tropospheric air are often much lower than methane, the importance of NMHCs is magnified by their high reactivity and by the multitude of reactions in which they participate in the atmosphere.[21] The agreement between this work and that of Rowley et al.[6] lends further support to the idea that the rate constants for reactions between larger peroxy radicals and HO_2 are enhanced compared to the reactivity of smaller peroxy radicals such as methyl and ethylperoxy. This may not have much of an effect in atmospheric models of urban areas with relatively high [NO]/[HO_2] ratios. However, in rural areas where peroxy radical reactions with NO are competitive with their reactions with HO_2 the reactivity differences between the "smaller" and "larger" peroxy radicals may become noticeable.

References and Notes

(1) Wallington, T. J.; Dagaut, P.; Kurylo, M. J. *Chem. Rev.* **1992**, *92*, 667.

(2) Lightfoot, P. D.; Cox, R. A.; Crowley, J. N.; Destriau, M.; Hayman, G. D.; Jenkin, M. E.; Moorgat, G. K.; Zabel, F. *Atmos. Environ.* **1992**, *26A*, 1805.

(3) Gery, M. W.; Whitten, G. Z.; Killus, J. P.; Dodge, M. C. *J. Geophys. Res.* **1989**, *94*, 12925.

(4) Carter, W. P. L. *Atmos. Environ.* **1990**, *24A*, 481.

(5) Rowley, D. M.; Lesclaux, R.; Lightfoot, P. D.; Hughes, K.; Hurley, M. D.; Rudy, S.; Wallington, T. J. *J. Phys. Chem.* **1992**, *96*, 7043.

(6) Rowley, D. M.; Lesclaux, R.; Lightfoot, P. D.; Noziere, B.; Wallington, T. J.; Hurley, M. D. *J. Phys. Chem.* **1992**, *96*, 4889.

(7) Boyd, A. A.; Lesclaux, R.; Jenkin, M. E.; Wallington, T. J. *J. Phys. Chem.* **1996**, *100*, 6594.

(8) Dagaut, P.; Wallington, T. J.; Kurylo, M. J. *J. Phys. Chem.* **1988**, *92*, 3833.

(9) Lightfoot, P. D.; Veyret, B.; Lesclaux, R. *J. Phys.Chem.* **1990**, *94*, 708.

(10) Dagaut, P.; Wallington, T. J.; Kurylo, M. J. *J. Phys. Chem.* **1988**, *92*, 3836.

(11) Fenter, F. F.; Catoire, V.; Lesclaux, R.; Lightfoot, P. D. *J. Phys. Chem.* **1993**, *97*, 3530.

(12) Maricq, M. M.; Szente, J. J. *J. Phys. Chem.* **1994**, *98*, 2078.

(13) Maricq, M. M.; Wallington, T. J. *J. Phys. Chem.* **1992**, *96*, 986.

(14) Maricq, M. M.; Szente, J. J. *J. Phys. Chem.* **1992**, *96*, 10862.

(15) Maricq, M. M.; Szente, J. J.; Kaiser, E. W. *J. Phys. Chem.* **1993**, *97*, 7970.

(16) Cattell, F. C.; Cavanagh, J.; Cox, R. A.; Jenkin, M. E. *J. Chem. Soc., Faraday Trans. 2* **1986**, *82*, 1999.

(17) Rowley, D. M.; Lightfoot, P. D.; Lesclaux, R.; Wallington, T. J. *J. Chem. Soc., Faraday Trans.* **1992**, *88*, 1369.

(18) DeMore, W. B.; Sander, S. P.; Golden, D. M. Hampson, R. F.; Kurylo, M. J.; Howard, C. J.; Ravishankara, A. R.; Kolb, C. E.; Molina, M. J. *Chemical Kinetics and Photochemical Data for Use in Stratospheric Modeling*; JPL Publication 94−26, 1994.

(19) Lightfoot, P. D.; Veyret, B.; Lesclaux, R. *J. Phys. Chem.* **1990**, *94*, 708.

(20) Wallington, T. J.; Skewes, L. M.; Siegl, W. O. *J. Phys. Chem.* **1989**, *93*, 3649.

(21) Greenberg, J. P.; Zimmerman, P. R.; Levine, J. S. *J. Geophys. Res.* **1984**, *89*, 4767.